Development of a 3-axis Parallel Kinematic Machine for Milling Wood Material – Part 1: Design

Elmas Aşkar Ayyıldız [a] and Mustafa Ayyıldız [b,*]

A 3-axis parallel kinematic machine tool and advanced control system with programming in G-code for the milling of wood material are described in detail. This parallel kinematic machine is based on a 3-PSS (prismatic link, spherical link, and spherical link) parallel mechanism. A programming system and control based on a real-time PC windows platform and Mach3 software system was implemented for this tool. Finally, a model application of a programming system developed for a three-degree-of-freedom linear delta parallel machine was presented, and the workability for milling wood material (medium-density fibreboard) was shown.

Keywords: Parallel kinematic machine; G-code; Milling wood material

*Contact information: a: Institute of Science and Technology, Karabük University, Karabük, Turkey; b: Manufacturing Engineering Department of Technology Faculty, Düzce University, Düzce, Turkey; *Corresponding author: mayyldz@hotmail.com*

INTRODUCTION

Wood machining is strongly influenced by wood texture. Thus, it is a very important field of research to achieve optimum wood machining conditions (Aguilera *et al.* 2000). Milling is a machining operation regularly used in manufacturing parts of wood. In previous literature, metal milling has been studied broadly, but medium-density fibreboard (MDF) milling has not received much attention. Many works (Aguilera *et al.* 2000; Gordon and Hillery 2003; Lin *et al.* 2006; Davim *et al.* 2009; Vančo *et al.* 2017), when reporting about the machining of wood material, have shown that the machinability is dependent upon the cutting tool, the cutting mechanics, and the workpiece material.

Parallel Kinematic Machines (PKMs) are frequently used in many industrial applications that require high precision demanded by the latest developments in technology. This is because parallel manipulators have such capabilities as a higher payload, high rigidity and accuracy, good stability, usability in high-speed applications, a good dynamic performance, and precise positioning. The PKMs are frequently employed in industrial applications such as medical operations, game simulators, oil platforms, heavy freight transport, light metal machining, polishing, cutting, shaping and assembly operations, and flight simulators.

Having reviewed the literature, Gao *et al*. (2002) presented a design and innovations for new variants of 2 degree-of-freedom (DOF), 3 DOF, 4 DOF, and 5 DOF parallel mechanisms. In their study, Liu *et al.* (2005) proposed the family of 3-degree-of-freedom parallel manipulators with a new high-revolution capacity to overcome low-revolution capabilities of existing parallel manipulators. Budde *et al.* (2007) presented design problems (singularity) and the optimization of a linear delta robot (workspace, rigidity, precision of varying rod lengths) and implemented their model application in furtherance of this work (Budde *et al.* 2008).

Stan *et al*. (2008) presented a multi-objective optimum design procedure to triglide and delta robot features, such as workspace boundaries, rigidity, and transmission quality index (speed, force, and power characteristics), which are the optimal design criteria for 3-DOF parallel robots. Corbel *et al*. (2008) presented the design and optimization of a parallel machine tool by combining a real 3-DOF robot (linear delta) with 6-DOF measuring parallel robots. Yuan *et al.* (2008) proposed optimal design methods for the linear delta robot to obtain a specified cuboid workspace.

Kelaiaia *et al.* (2012) presented an illustrative application of the methodology developed for a linear delta parallel robot with 3-DOF. This methodology involves the geometric, kinematic, and dynamic models of the selected structure. It estimates performance criteria (workspace, rigidity, kinematic, and dynamic performance), determines the boundaries of the robot structure, creates mathematical formulae of the optimization problem, and uses a genetic algorithm utility for the solution of the problem. Patel and George (2012) compared various criteria, such as structures and workspaces, for serial and parallel manipulators. Niu *et al.* (2013) presented the dynamics and control of a novel 3-DOF parallel manipulator with actuation redundancy. Zeng *et al.* (2014) introduced the structure and constraint design of a 3-DOF translational parallel manipulator. Lin *et al.* (2015) investigated the design and implementation of the delta parallel robot, covering the entire mechatronic process, involving kinematics, control design, and optimizing methods. Xie *et al.* (2016) proposed a 6-DOF hybrid mechanism for the development of a turbine blade grinding machine. The conceptual design was presented, and the singularity of the 3-DOF parallel module was analyzed. Xu *et al.* (2017) presented a novel hybrid machine with 6-DOF serial-parallel topological structure used as an ultra-precision polishing equipment.

Today, the majority of university laboratories, research institutes, and enterprises do not have PKMs. This is because education and training costs for a novel technology like PKM are high. There are rare studies in the literature on a low-cost 3-DOF parallel kinematic machine aimed at contributing to practical experiences in the use of PKM (Glavonjic *et al*. 2009). Yang and Hong (2001) developed a real-time intercept-based three-dimensional (3D) linear and circular interpolation software to achieve simultaneous 3-axis motion on the PC-NC milling machine. Gordon and Hillery (2005) developed a low-cost bridge-type X/Y motion system. In this system, the CNC controller is controlled by an interface that supports G-codes written in C ++. Kanaan *et al.* (2009) obtained inverse and forward kinematic equations for a serial-parallel 5-axis machine, which they called a VERNE machine tool. Here, symbolic methods to calculate all kinematic solutions are proposed.

Guo *et al.* (2012) developed a universal numeric control (NC) program processor for CNC systems aimed at processing various types of NC software because most CNC manufacturers use their own custom functions in NC software. In this study, the purpose is to transform the G-codes produced by any CAM software for controlling a linear delta parallel machine, one of the PKM structures, into a new G-code structure interpretable by the robot. For this purpose, an inverse kinematic model was developed for the linear delta parallel machine, and G-codes were transformed into a meaningful code system for this structure through a designed interface. The new codes produced were transferred to the PKM structure in a sequence to control the system.

EXPERIMENTAL

Description and Kinematics of the Mechanism

Figure 1 shows the geometric definitions for the linear delta parallel machine. As can be seen in Fig. 2, the machine is in the form of a 3-degree-of-freedom parallel robot of 3-PSS (prismatic link, spherical link, spherical link) type (Gao *et al*. 2002). The robot consists of arms integrated into the fixed platform and a mobile platform. The mobile platform and the fixed platform are coupled to each other by 3 kinematic chains arranged at an angle of α_i. Each kinematic chain was jointed with 2 parallel rods of length L (with a distal and proximal spherical link) and with a linear actuator (Gao *et al*. 2002).

The mobile platform always remained parallel to the fixed platform. The prismatic motion of the mobile platform was provided by the combined motion of all 3 actuators. In the literature, there are various studies on the kinematic modeling of a linear delta robot (Company and Pierrot 2002; Righettini *et al.* 2002; Liu *et al.* 2004; Kelaiaia *et al.* 2012; Xie *et al.* 2016).

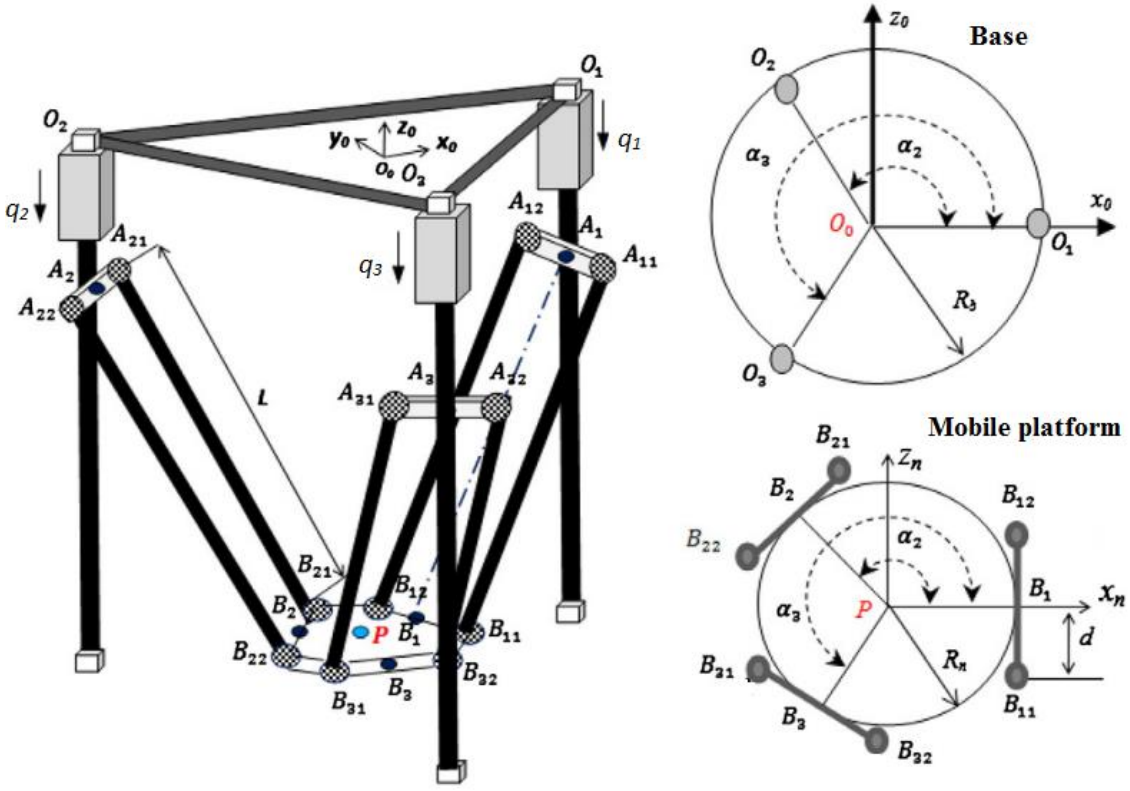

Fig. 1. Geometric definition of the linear delta robot (Gao *et al*. 2002)

The geometric definitions of the linear delta robot are given below (Gao *et al*. 2002),

$\{R_0\}$: (0_0--x_0, y_0, z_0): "0_0" is the reference frame for the fixed platform, the center of the equilateral triangle $0_10_20_3$, and also the center of the circle with radius R_b.

$\{R_p\}$: (P—x_n, y_n, z_n): "P" is the reference frame for the mobile platform, the center of the equilateral triangle $B_1B_2B_3$, and also the center of the circle with radius R_n.

q_1, q_2, q_3: Links the variables for stroke control of 3 linear actuators.

R_b: Is the radius of the circle centered at 0_0, and the distance between 0_i and 0_0, and $\|0_00_i\| = R_b, i = 1,2,3$

R_n: Is the radius of the circle centered at *P*, the distance between "*P*",B_i, and the center of the mobile platform, and $\|PB_i\| = R_n, i = 1,2,3$.

The kinematic model for the linear delta robot refers to the position and the orientation of the end effector in relation to the reference frame (R_0) and $\|A_iB_i\| = L$.

$$A_iB_i^2 - L^2 = 0,\ i = 1, 2, 3 \quad (1)$$

Coordinates of B_i in the reference frame for the movable platform are given in Eq. 2,

$$[B_i]_{sabit} = \begin{bmatrix} x + R_n cos\alpha_i \\ y + R_n sin\alpha_i \\ z \end{bmatrix} \quad (2)$$

and coordinates of A_i in the reference frame for the fixed platform are given in Eq. 3,

$$[A_i]_{sabit} = \begin{bmatrix} R_b cos\alpha_i \\ R_b sin\alpha_i \\ q_i \end{bmatrix} \quad (3)$$

$$\alpha_i = \frac{2\pi}{3}(i-1),\ i = 1,2,3 \quad (4)$$

Using Eq. 1 to build the expression of the inverse kinematic model, Eq. 5 was obtained.

$$q_i = z + \sqrt{L^2 - (x - (R_b - R_n)cos\alpha_i)^2 - (y - (R_b - R_n)sin\alpha_i)^2} \quad (5)$$

To build the forward kinematic model for the linear delta robot, Eq. 6 should be solved with respect to X, Y, and Z (Stan *et al.* 2008),

$$\begin{Bmatrix} Fz^2 + 2Gz + H = 0 \\ y = Az + B \\ x = Cz + D \end{Bmatrix} \quad (6)$$

where:

$$z_{1,2} = \frac{-2G \pm \sqrt{2G^2 - 4FH}}{2F} \quad (7)$$

The solution adopted was $z = \min(z_1, z_2)$

$$A = \frac{(q_2 - q_3)}{\sqrt{3}(R_b - R_n)} \quad (8)$$

$$B = \frac{{q_3}^2 - {q_2}^2}{2\sqrt{3}(R_n - R_b)} \quad (9)$$

$$C = \frac{2(q_2 - q_1) - A(R_n - R_b)\sqrt{3}}{3(R_b - R_n)} \quad (10)$$

$$D = \frac{{q_1}^2 - {q_2}^2 - B\sqrt{3}(R_n - R_b)}{3(R_b - R_n)} \quad (11)$$

$$E = (R_n - R_b) + B \quad (12)$$

$$F = A^2 + C^2 + 1 \quad (13)$$

$$G = AE + CD - q_1 \quad (14)$$

$$H = E^2 + D^2 + {q_1}^2 - L^2 \quad (15)$$

Applying the above equations to Eq. 6, the forward kinematic model for the linear delta robot was formulated.

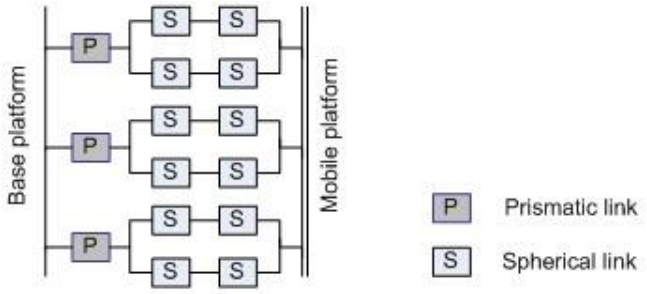

Fig. 2. Link scheme for the linear delta robot

Control Structure of Linear Delta Parallel Machine

Integrated operations of the system were ensured *via* a software system appropriate for controlling the linear delta parallel machine. The interface designed with an inverse kinematic modeling of linear delta and G-codes were transformed into a meaningful code system for this structure. The codes produced were transferred to the PKM structure in a sequence to control the system. Figure 3 shows the control structure of the linear delta parallel machine.

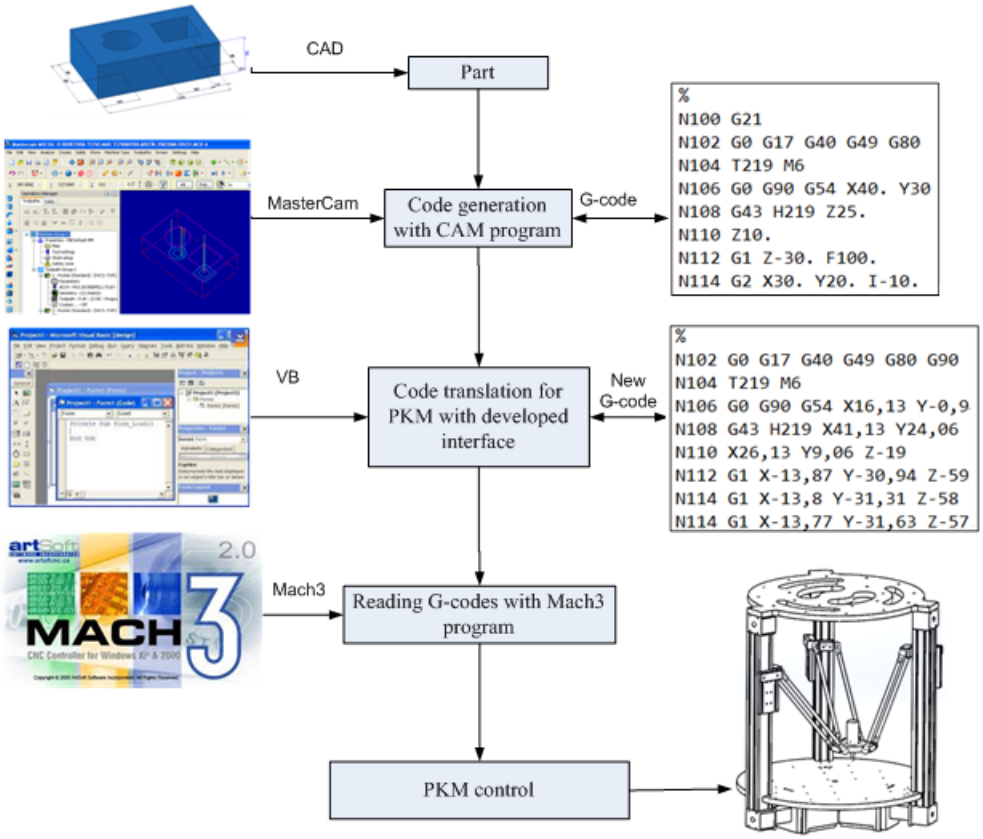

Fig. 3. Control flowchart of the linear delta parallel machine

Based on Fig. 3, it is possible to plan the orbit of the linear delta parallel machine. By designing the model of any physical object, the object's build codes were produced

with the help of the CAM software. Here, build codes produced with the CAM software were formed according to the Cartesian space. Adapting these codes in the Cartesian space to the build environment, motors linked to the X, Y, and Z axes were linearly driven. The codes produced for the Cartesian structure were not suitable for the motional structure of the linear delta parallel machine structure within the workspace. Due to the linear motion of the arms A_1, A_2, and A_3 of the linear delta, and due to the prismatic motions occurring at the joint of these arms, transformation into a coding system interpretable by the Cartesian structure was necessary. Therefore, a new code system was created based on appropriate CAM codes through an interface according to the prismatic motion of arms A_1, A_2, and A_3 by linear delta, and by employing the kinematic equations for this structure. The new codes produced were run on the Mach3 software (Valentino and Goldenberg 2006) for controlling the linear delta parallel machine. Control of the linear delta parallel machine was conducted by repeating this sequence.

RESULTS AND DISCUSSION

Producing CAM Codes

Using the Mastercam X5 software (Valentino, and Goldenberg 2006), the build codes of an object designed in any CAD software were produced. In producing the build codes with Mastercam X5, the machine type selected was "Default". The reason for this is that there is no machine type available for the linear delta parallel machine. Figure 4 shows a sample code produced with Mastercam X5.

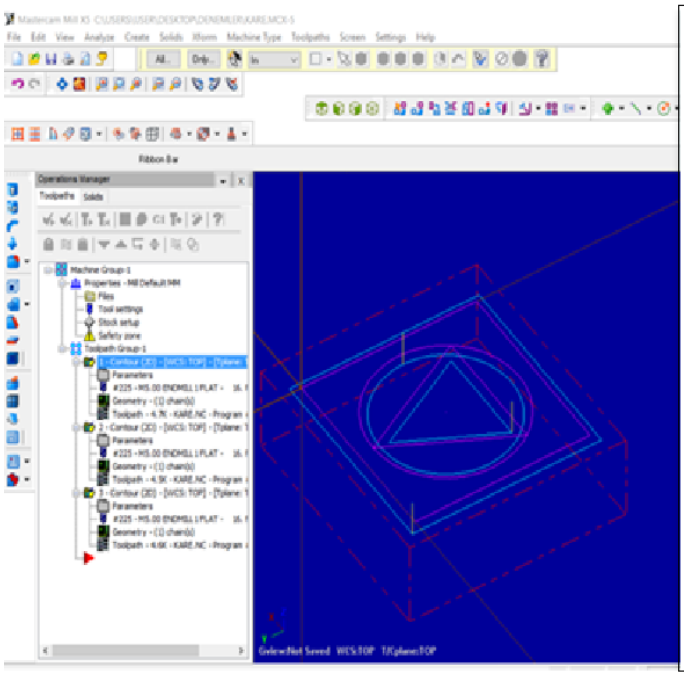

```
%
N100 G21
N102 G0 G17 G40 G49 G80 G90
N104 T219 M6
N106 G0 G90 G54 X40. Y30. A0. S1500 M3
N108 G43 H219 Z25.
N110 Z10.
N112 G1 Z-5. F100.
N114 G2 X30. Y20. I-10. J0. F50.
N116 X20. Y30. I0. J10.
N118 X30. Y40. I10. J0.
N120 X40. Y30. I0. J-10.
N122 G1 X35.625
N124 X34.677 Y26.875
N126 X32.577 Y25.
N128 X27.423
N130 X24.961 Y27.5
N132 X24.41 Y30.625
N134 X25.807 Y33.75
N136 X27.423 Y35.
N138 X32.577
N140 X35.039 Y32.5
N142 X35.625 Y30.
N144 G0 Z20.
N146 X40.
N148 Z5.
```

Fig. 4. Sample code produced with Mastercam X5

Code Transformation with the Interface Developed

Because the codes produced with Mastercam X5 in Fig. 4 were appropriate for machine types of the Cartesian structure, these codes were transformed into the motion

space of the parallel delta parallel machine that had a parallel structure. The inverse kinematic equations were employed. The interface was developed in Visual Studio 2015 (Fig. 5).

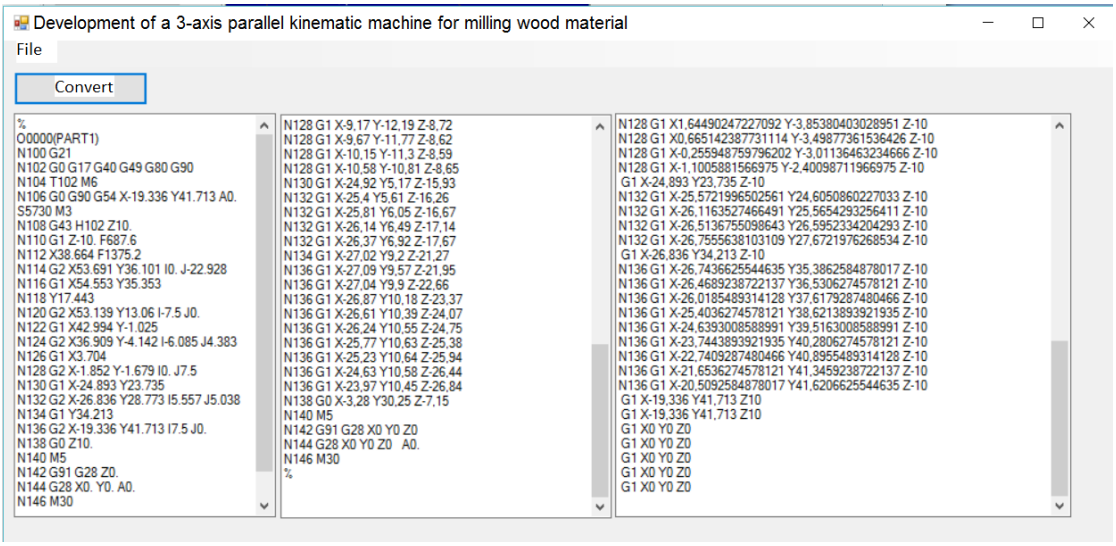

Fig. 5. The interface developed

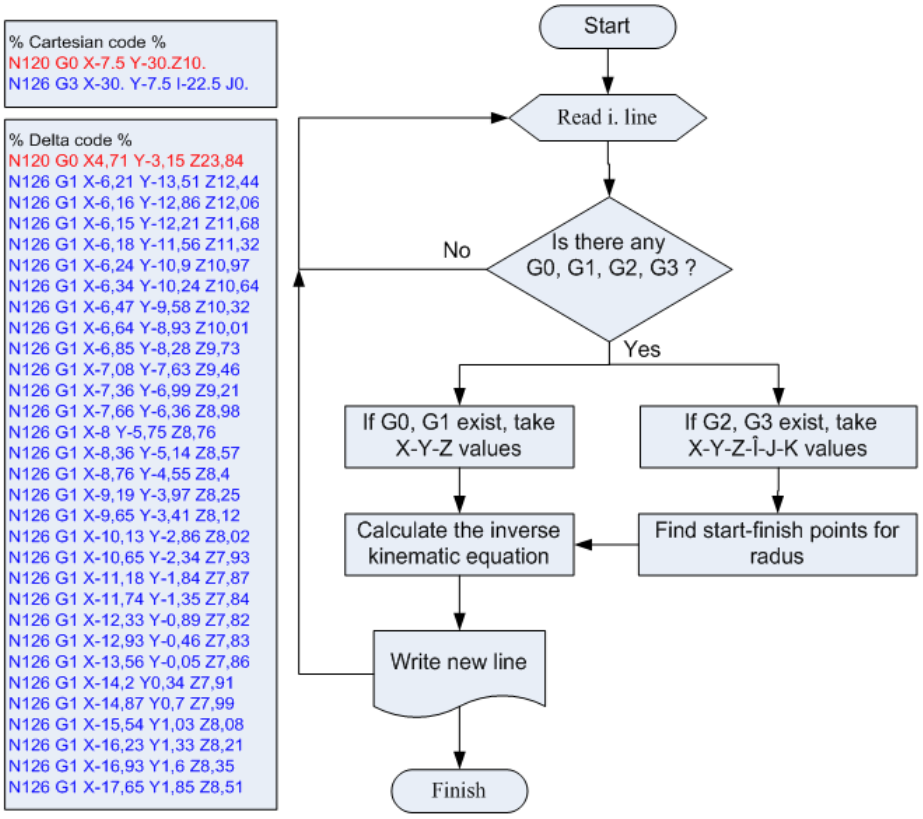

Fig. 6. Flowchart of the interface system developed

The flowchart of the interface system developed is shown in Fig. 6. In this interface, an algorithm was developed for codes G0, G1, G2, and G3. For codes G0 and G1, a new

code was produced by performing an inverse kinematic calculation with X, Y, Z values in the corresponding row. Using the start and end points of the arc as a reference for the code G2, the arc path was pixelated for a clockwise linear interpolation with X, Y, Z and I, J, K values. These pixels were calculated based on the arc angle and hypotenuse found. The same applied to code G3. When the interface recognized the codes G2 and G3, the algorithm ran and the new code was transformed as a code G1. Figure 7 shows G2 and G3 circular interpolation parameters (Petrovic *et al.* 2017).

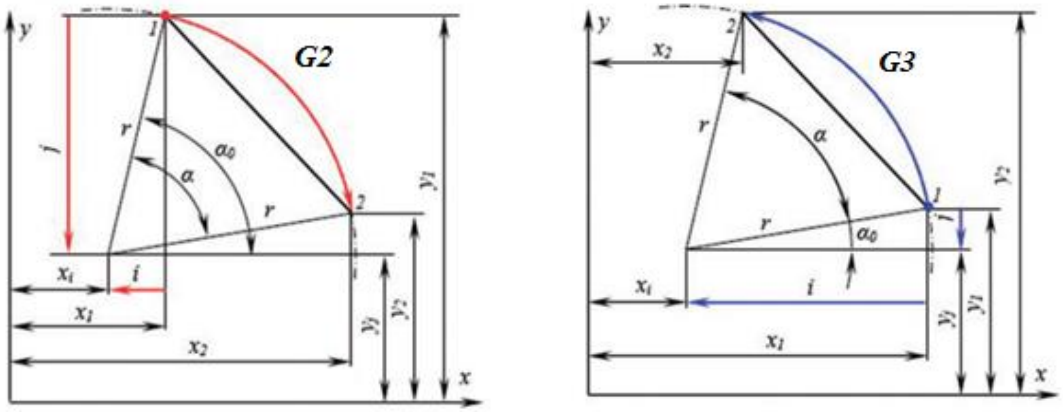

(a) (b)

Fig. 7. G2 and G3 circular interpolation parameters

The radius of the arcs shown in Fig. 7 is given in Eq. 16, while the arc angles are given in Eqs. 17 and 18 (Petrovic *et al.* 2017),

$$r = \sqrt{i^2 + j^2} \quad , \quad x_c = x_1 + i; \quad y_c = y_1 + j \tag{16}$$

$$\alpha_0 = \left| \text{arctg}\left(\frac{y_1 - y_c}{x_1 - x_c} \right) \right|; \quad \alpha_0 = \begin{cases} \alpha_0, y_1 - y_c \geq 0 \wedge x_1 - x_c \geq 0 \\ 180 - \alpha_0, y_1 - y_c \geq 0 \wedge x_1 - x_c < 0 \\ 180 + \alpha_0, y_1 - y_c < 0 \wedge x_1 - x_c < 0 \\ 360 - \alpha_0, y_1 - y_c < 0 \wedge x_1 - x_c \geq 0 \end{cases} \tag{17}$$

$$\alpha_1 = \left| \text{arctg}\left(\frac{y_2 - y_c}{x_2 - x_c} \right) \right|; \quad \alpha_1 = \begin{cases} \alpha_1, y_2 - y_c \geq 0 \wedge x_2 - x_c \geq 0 \\ 180 - \alpha_1, y_2 - y_c \geq 0 \wedge x_2 - x_c < 0 \\ 180 + \alpha_1, y_2 - y_c < 0 \wedge x_2 - x_c < 0 \\ 360 - \alpha_1, y_2 - y_c < 0 \wedge x_2 - x_c \geq 0 \end{cases} \tag{18}$$

where x_1, y_1, and z_1 are the arc start coordinates, x_2, y_2, and z_2 are the arc end coordinates, x_c, y_c, and z_c are central coordinates of the circular interpolation, r is the radius of the circular interpolation (°), α_0 is the start angle of the circular interpolation (°), and α_1 is the circular interpolation angle (°).

Running New Codes with Mach3

The new codes produced were run using the Mach3 software. The Mach3 software communicated with the AKZ250 USB control card to guide the motors. As practice, the contouring of square, circle, and triangle geometries was performed. Figure 8 shows a model application. Table 1 shows the G-codes produced for the Cartesian structure, and the new G-codes transformed into a delta structure through the interface developed.

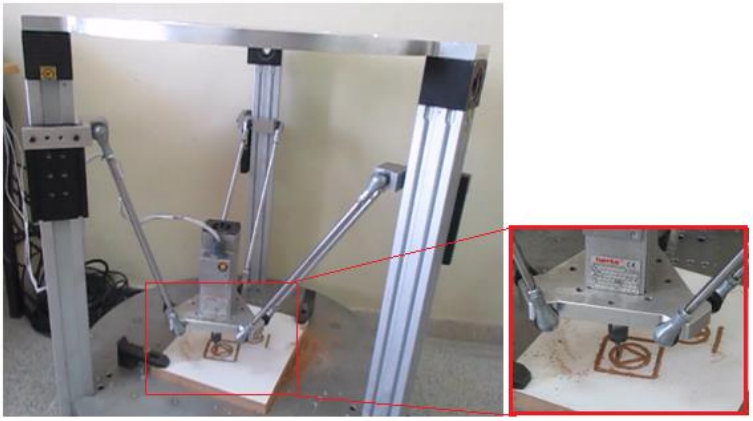

Fig. 8. Model contouring for a square, circle, and triangle

Table 1. The G-codes Produced for the Cartesian Structure

Cartesian G-codes	G-codes for Delta Structure
% O0000(TUM) N102 G0 G17 G40 G49 G80 G90 N104 T225 M6 N106 G0 G90 G54 X-62.5 Y2.5. S5730 M3 N108 G43 H225 Z10. N110 G1 Z-1. F859.5 N112 X2.5 F250. N114 Y-62.5 N116 X-62.5 N118 Y2.5 N120 G0 Z10. N122 X-7.5 Y-30. N124 G1 Z-1. F859.5 N126 G3 X-30. Y-7.5 I-22.5 J0. F250. - - - - N154 M30 %	% O0000(TUM) N102 G0 G17 G40 G49 G80 G90 N104 T225 M6 N106 G0 G90 G54 X-30,29 Y21,67 Z19,48 S5730 M3 N108 G43 H225 X-30,29 Y21,67 Z19,48 N110 G1 X-41,29 Y10,67 Z8,48 F859.5 N112 X0,28 Y-0,54 Z-2,8 F250. N114 X-5,24 Y-37,14 Z20,33 N116 X-47,55 Y-24,69 Z30,94 N118 X-41,29 Y10,67 Z8,48 N120 G0 X-30,29 Y21,67 Z19,48 N122 X4,71 Y-3,15 Z23,84 N124 G1 X-6,29 Y-14,15 Z12,84 F859.5 N126 G1 X-6,21 Y-13,51 Z12,44 F250 N126 G1 X-6,16 Y-12,86 Z12,06 N126 G1 X-6,15 Y-12,21 Z11,68 N126 G1 X-6,18 Y-11,56 Z11,32 N126 G1 X-6,24 Y-10,9 Z10,97 N126 G1 X-6,34 Y-10,24 Z10,64 N126 G1 X-6,47 Y-9,58 Z10,32 N126 G1 X-6,64 Y-8,93 Z10,01 N126 G1 X-6,85 Y-8,28 Z9,73 - - - N154 M30 %

CONCLUSIONS

1. This paper introduced a novel design of a linear delta parallel machine for milling wood material. The development of the machine involved the development of the mechanism, as well as both its hardware and software.
2. An inverse kinematic model was developed for the linear delta parallel machine, and G-codes were transformed into a meaningful code system for this structure through the designed interface. The new codes produced were transferred to the linear delta structure in a sequence to control the system.
3. Finally, by developing a model application of a programming system developed for a 3 degree-of-freedom linear delta parallel machine, the workability for milling wood material (medium-density fibreboard) was shown.

REFERENCES CITED

Aguilera, A., Meausoone, P. J., and Martin, P. (2000). "Wood material influence in routing operations: The mdf case," *Eur. J. Wood Wood Prod.* 58(4), 278-283. DOI: 10.1007/s001070050425

Budde, C., Last, P., and Hesselbach, J. (2007). "Development of a triglide-robot with enlarged workspace," in: *Robotics and Automation 2007 IEEE International Conference*, Rome, Italy, pp. 543-548.

Budde, C., Rose, M., Maass, J., and Raat, A. (2008). "Automatic detection of assembly mode for a Triglide-robot," in: *Robotics and Automation 2008 IEEE International Conference*, Pasadena, CA, USA, pp. 1568-1575.

Company, O., and Pierrot, F. (2002). "Modelling and preliminary design issues of a 3-axis parallel machine-tool," *Mech. Mach. Theory* 37(11), 1325-1345. DOI: 10.1016/S0094-114X(02)00040-X

Corbel, D., Company, O., and Pierrot, F. (2008). "Optimal design of a 6-dof parallel measurement mechanism integrated in a 3-dof parallel machine-tool," in: *Intelligent Robots and Systems 2008 IEEE/RSJ International Conference*, Nice, France, pp. 1970-1976.

Davim, J. P., Clemente, V. C., and Silva, S. (2009). "Surface roughness aspects in milling MDF (medium density fibreboard)," *Int. J. Adv. Manuf. Tech.* 40(1), 49-55. DOI: 10.1007/s00170-007-1318-z

Gao, F., Li, W., Zhao, X., Jin, Z., and Zhao, H. (2002). "New kinematic structures for 2-, 3-, 4-, and 5-dof parallel manipulator designs," *Mech. Mach. Theory* 37(11), 1395-1411.DOI: 10.1016/S0094-114X(02)00044-7

Glavonjic, M., Milutinovic, D., and Zivanovic, S. (2009). "Functional simulator of 3-axis parallel kinematic milling machine," *Int. J. Adv. Manuf. Tech.* 42(7), 813-821. DOI: 10.1007/s00170-008-1643-x

Gordon, S., and Hillery, M. T. (2003). "A review of the cutting of composite materials," *P. I. Mech. Eng. L-J. Mat.* 217(1), 35-45. DOI: 10.1177/146442070321700105

Gordon, S., and Hillery, M. T. (2005). "Development of a high-speed CNC cutting machine using linear motors," *J. Mater. Process. Tech.* 166(3), 321-329. DOI: 10.1016/j.jmatprotec.2003.08.009

Guo, X., Liu, Y., Du, D., Yamazaki, K., and Fujishima, M. (2012). "A universal NC program processor design and prototype implementation for CNC systems," *Int. J. Adv. Manuf. Tech.* 60(5), 561-575. DOI: 10.1007/s00170-011-3618-6

Kanaan, D., Wenger, P., and Chablat, D. (2009). "Kinematic analysis of a serial–parallel machine tool: The verne machine," *Mech. Mach. Theory* 44(2), 487-498. DOI: 10.1016/j.mechmachtheory.2008.03.002

Kelaiaia, R., Company, O., and Zaatri, A. (2012). "Multiobjective optimization of a linear delta parallel robot," *Mech. Mach. Theory* 50, 159-178. DOI: 10.1016/j.mechmachtheory.2011.11.004

Lin, J., Luo, C. H., and Lin, K. H. (2015). "Design and implementation of a new delta parallel robot in robotics competitions," *Int. J. Adv. Robot Syst.* 12(10), 153-162. DOI: org/10.5772/61744

Lin, R. J., Van Houts, J., and Bhattacharyya, D. (2006). "Machinability investigation of medium-density fibreboard," *Holzforschung* 60(1), 71-77. DOI: 10.1515/HF.2006.013

Liu, X. J., Wang, J., and Pritschow, G. (2005). "A new family of spatial 3-dof fully-parallel manipulators with high rotational capability," *Mech. Mach. Theory* 40(4), 475-494. DOI: 10.1016/j.mechmachtheory.2004.10.001

Liu, X. J., Wang, J., Oh, K. K., and Kim, J. (2004). "A new approach to the design of a delta robot with a desired workspace," *J. Intell. Robot. Syst.* 39(2), 209-225. DOI: 10.1023/B:JINT.0000015403.67717.68

Niu, X. M., Gao, G. Q., Liu, X. J., and Bao, Z. D. (2013). "Dynamics and control of a novel 3-DOF parallel manipulator with actuation redundancy," *Int. J. Autom. Comput.* 10(6), 552-562. DOI: org/10.1007/s11633-013-0753-6

Patel, Y. D., and George, P. M. (2012). "Parallel manipulators applications—a survey," *Modern Mechanical Engineering* 2(3), 57-64. DOI: 10.4236/mme.2012.23008

Petrovic, A., Lukic, L., Ivanovic, S., and Pavlovic, A. (2017). "Optimisation of tool path for wood machining on CNC machines," *P. I. Mech. Eng. C-J. Mec.* 231(1), 72-87. DOI: 10.1177/0954406216648715

Righettini, P., Tasora, A., and Giberti, H. (2002). "Mechatronic design of a 3-dof parallel translational manipulator," in: *11th International on Robotics in Alpe-Adria-Danube Region*, Balatonfured, Hungary, pp. 367-372.

Stan, S. D., Manic, M., Maties, V., and Balan, R. (2008). "Evolutionary approach to optimal design of 3 DOF translation exoskeleton and medical parallel robot," in: *Human System Interactions 2008 Conference*, Krakow, Poland, pp. 720-725.

Valentino, J., and Goldenberg, J. (2006). "Learning mastercam x5 mill 2d step-by-step," Industrial Press Inc., New York, USA.

Vančo, M., Jamberová, Z., Barcík, Š., Gaff, M., Čekovská, H., and Kaplan, L. (2017). "The effect of selected technical, technological, and material factors on the size of juvenile poplar wood chips generated during face milling," *BioResources* 12(3), 4881-4896. DOI: 10.15376.biores./12.3.4881-4896

Xie, F., Liu, X. J., and Wang, J. (2016). "Conceptual design and optimization of a 3-DoF parallel mechanism for a turbine blade grinding machine," *P. I. Mech. Eng. C-J. Mec.* 230(3), 406-413. DOI: 10.1177/0954406215589122

Xu, P., Li, B., Cheung, C. F., and Zhang, J. F. (2017). "Stiffness modeling and optimization of a 3-DOF parallel robot in a serial-parallel polishing machine," *Int. J. Precis. Eng. Man.* 18(4), 497-507. DOI: org/10.1007/s12541-017-0060-1

Yang, M. Y., and Hong, W. P. (2001). "A PC–NC milling machine with new simultaneous 3-axis control algorithm," *Int. J. Mach. Tool. Manu.* 41(4), 555-566. DOI: 10.1016/S0890-6955(00)00091-2

Yuan, Q., Ji, S., Wang, Z., Wang, G., Wan, Y., and Zhan, L. (2008). "Optimal design of the linear delta robot for prescribed cuboid dexterous workspace based on performance chart," in: *WSEAS International Conference Proceedings Mathematics and Computers in Science and Engineering (No. 8) World Scientific and Engineering Academy and Society*, Hangzhou, China, pp. 35-41.

Zeng, Q., Ehmann, K. F., and Cao, J. (2014). "Tri-pyramid robot: design and kinematic analysis of a 3-DOF translational parallel manipulator," *Robot Comput. Integr. Manuf.* 30(6), 648-657. DOI: org/10.1016/j.rcim.2014.06.002

Article submitted: June 23, 2017; Peer review completed: October 14, 2017; Revised version received and accepted: October 18, 2017: Published: October 25, 2017.
DOI: 10.15376/biores.12.4.9326-9337